Paradoxical Changes of Cutaneous Microcirculation and Sympathetic Fibers of Rat Hind Limbs after Sciatic Nerve Compression

Yi Peng, MD
Junren Lu, PhD
Shunyi Lu, MD
Jiapeng Zou, PhD
Tengfei Fu, PhD
Libo Jiang, PhD
Jiayi Wang, PhD
Dehua Meng, PhD
Zenggan Chen, PhD
Jian Zhang, PhD

Shanghai, People's Republic of China

Background: Recent studies show evidence that surgical nerve decompression could improve cutaneous blood flow (CBF), which might benefit ulcer healing. However, the change of CBF and sympathetic fibers after nerve compression is poorly understood. In the current study, a unilateral sciatic nerve compression model was created in Sprague-Dawley rats.
Methods: A laser Doppler imaging system was applied to assess the CBF of the regions below the ankles. Immunohistochemistry and transmission electron microscopy were used to investigate the histopathologic changes of sympathetic fibers in sciatic nerve samples.
Results: Laser Doppler imaging revealed decreased CBF of both the lesional limb and the contralesional limb, which occurred earlier in the lesional side, indicating an enhanced sympathetic tone on vasomotor function. Intraneural density of sympathetic fibers decreased on both sides and the ultrastructure of unmyelinated fibers of both sides degenerated in a nonsynchronized manner.
Conclusions: The study revealed nonsynchronized reduced CBF of bilateral hind limbs with paradoxically degenerated and diminished sympathetic fibers in bilateral sciatic nerves after unilateral sciatic nerve compression. These results may validate the importance of and broaden the indications for surgical nerve decompression in preventing or treating foot ulcers. *(Plast. Reconstr. Surg.* 151: 245e, 2023.)

Nerve compression, or entrapment neuropathy, is a common disease of the peripheral nervous system, including carpal tunnel syndrome, tarsal tunnel syndrome, cubital tunnel syndrome, and pyriformis syndrome. It commonly manifests as paresthesia or neuralgia, sensory loss, muscular atrophy, and electrophysiologic changes or autonomic symptoms, such as abnormal color and temperature of skin, hyperhidrosis, or hypohidrosis.[1–4]

Autonomic dysfunction has been relatively less studied because it has been regarded as less harmful. Neuropathy of sympathetic fibers, an important component of autonomic fibers, may play a role under certain circumstances. Studies have shown that nerve compression is more prevalent in the diabetic population,[5] which can lead to further deterioration in diabetic peripheral neuropathy. Diabetic peripheral neuropathy–related foot deformity, sensation loss, and dry skin are considered to be the cardinal pathologic processes in the development of foot ulceration and its recurrence.[6] This theory remains inadequate to explain accelerated wound healing after surgical nerve decompression,[7,8] as the relief of motor, sensory, and sweating function is conducive to preventing progression and reducing recurrence

From the Department of Orthopaedics, Zhongshan Hospital, Fudan University.
Received for publication January 9, 2021; accepted February 2, 2022.
The first three authors contributed equally to this work.

DOI: 10.1097/PRS.0000000000009842

Disclosure: *Dr. Zhang received financial support from the National Natural Science Foundation of China (grant 81870965) for this article. The other authors have no financial interests to report.*

Related digital media are available in the full-text version of the article on www.PRSJournal.com.

of ulcers in the long term,[9–13] versus improving wound healing in the short term. Using transcutaneous oximetry, the cutaneous microcirculation was found to be markedly improved after surgical nerve decompression,[14] indicating a relation between cutaneous microcirculation and nerve compression.

To our knowledge, changes in cutaneous microcirculation and the sympathetic fibers in nerve compression diseases are poorly explained. This study aimed to explore the effect of peripheral nerve compression on the cutaneous microcirculation and sympathetic fibers.

METHODS AND MATERIALS

Male Sprague-Dawley rats weighing ≈250 g were used in the study. All experimental procedures involving animals were approved by the Institutional Animal Care and Use Committee of Fudan University (Shanghai, People's Republic of China). Every measure was taken to minimize the number of animals used and their discomfort. Rats were housed in a temperature- and humidity-controlled room (temperature 22 ± 2°C, humidity 55% ± 5%) and fed standard rat chow and water ad libitum, with a 12-hour:12-hour light–dark cycle.

No diabetes induced; ??level of pressure achieved?

Surgical Procedure

Thirty-two rats were randomly assigned to a nerve compression group or a sham operation group. All surgical procedures were performed under aseptic conditions. The rats were anesthetized in an isoflurane chamber (3%; 0.5 L/min) before intraperitoneal injection of pentobarbital (40 mg/kg). After anesthesia administration, each rat was placed in prone position with hind limbs stretched and its skin was wiped with 75% alcohol three times before the operation. The sciatic nerve of the left hind limb was exposed through a gluteal-splitting approach. In the compression group, once the sciatic nerve was identified and dissected, a 10-mm length, 0.8-mm inner diameter sterile silicone tube was wrapped circumferentially around the middle third of the nerve and fastened gently with 8-0 sutures. The edges of the silicone tube did not overlap or leave any space to obtain the desired degree of compression. The tube was able to glide along the nerve when dragged gently using forceps and the perineural blood flow was assessed visually to avoid obstruction. [**See Figure, Supplemental Digital Content 1**, which shows (*left*) intraoperation of nerve compression. The edges of the silicone tube did not overlap or leave any space to obtain the desired degree of compression. The tube was able to glide along the nerve when dragged gently using forceps and the perineural blood flow was assessed visually to avoid obstruction. (*Right*) During the laser Doppler imaging scanning, the rat was placed in supine position, with hind paws fixed on a black cushion. Both of the hind limbs were scanned simultaneously (*solid line frame*). The regions below the ankles (*dotted line frame*) were selected as the region of interest, ***http://links.lww.com/PRS/F573***.] This step was performed under the microscope to ensure the appropriate pressure, and the incision was then closed. In the sham-operation group, the nerve was returned to the host bed after dissection without any traumatic manipulation. All the procedures were performed by the same investigator to exclude manual influence.

Cutaneous Microcirculation Assessment

A PeriScan PIM III system (Perimed AB; Järfälla, Sweden) was used to measure skin blood flow of the hind limbs at 1, 2, 4, and 8 weeks after the surgical procedure. The PeriScan system uses laser Doppler perfusion imaging to detect moving blood cells in the blood flow, reflecting the perfusion of the skin by both color image and numerical value.

After receiving anesthesia, each rat was placed under the scanner in a supine position, with hind paws fixed on a black cushion. Both of the hind limbs were scanned simultaneously. The regions below the ankles were selected as the regions of interest and quantified for average perfusion with PIMSoft Version 1.5.4.8078 (Perimed AB) (**see Figure, Supplemental Digital Content 1**, ***http://links.lww.com/PRS/F573***). The range of the color scale was set to the default value of 0 to 300.

Histology and Immunohistochemistry

At 2, 4, and 8 weeks after the surgery, the rats were killed by an overdose of anesthesia. The surgical segment of sciatic nerve and approximately 1 cm of the contralateral sciatic nerve were harvested. The samples were fixed with 4% paraformaldehyde to make paraffin 3-μm-thickness sections. The sections were then immunostained using anti–dopamine β-hydroxylase antibody (1:50, ab209487, Abcam, U.K.) to elucidate sympathetic fibers at 4°C overnight after having been blocked by 5% milk in Tris-buffered saline for 30 minutes. Sections were subsequently washed in Tris-buffered saline three times and then exposed to anti-rabbit secondary antibody (Guge Biology

Technology Company, Wuhan, People's Republic of China) for 60 minutes.

For each section (one section per sample) of the nerve samples, four random high-power fields (400×) were captured and processed using ImageJ software (National Institutes of Health; Bethesda, MD). The semiquantitative density of sympathetic fibers was expressed as percentage of the dopamine β-hydroxylase–positive staining area in relation to the total area of the nerve in the visual field.[15,16]

Transmission Electron Microscopy

A 1-mm-length segment of each sciatic nerve specimen was cut and fixed in transmission electron microscopy fixative (G1102; Servicebio, Wuhan, People's Republic of China) overnight. After fixation, samples were washed with 0.1 M phosphate-buffered saline (pH 7.4) three times, postfixed in 1% osmium tetroxide for 2 hours in room temperature, and then embedded in resin according to standard protocols after alcohol dehydration. Ultrathin transverse sections (50-nm thickness) were stained with uranyl acetate and lead citrate and were observed with a transmission electron microscope (H-600; Hitachi, Tokyo, Japan). For morphometric analysis (semithin sections), photographed images were analyzed using ImageJ software by an observer blinded to the experimental design. The unmyelinated fibers were recognized by their appearance of multiple axons ensheathing within one Schwann cell, which is also known as Remak cell. The diameter of each unmyelinated axon was measured using ImageJ software. The length of the shorter axis was recorded when the axon presented as an oval, a column, or an irregular shape.

Statistical Analysis

GraphPad Prism 7 (GraphPad Software, San Diego, CA) was used to analyze data. Experimental data were expressed as mean ± standard error of the mean. Shapiro-Wilk test was conducted to evaluate the normality of data. For data with normal distribution, results between groups were compared by one-way analysis of variance with Bonferroni post hoc correction. Results between the operated and nonoperated limbs in the same group were compared by paired *t* test. For data that do not conform to normal distribution, results between groups were compared by Kruskal-Wallis test with Dunn post hoc comparison. Results between the operated and nonoperated limbs in the same group were compared by Wilcoxon signed rank test. A *P* value lower than 0.05 was considered statistically significant.

RESULTS

Cutaneous Blood Flow of Bilateral Hind Limbs Decreased after Sciatic Nerve Compression

Laser Doppler imaging was used to determine changes in cutaneous blood flow (CBF) of the regions below the ankles, which were selected as the region of interest. One week after the surgery, in the nerve compression group, laser Doppler imaging revealed a considerably reduced CBF of the lesional limb compared with the contralesional limb (220.2 ± 24.06 versus 301.0 ± 41.55; $P = 0.0099$) and sham-operated limb (220.2 ± 24.06 versus 389.9 ± 49.7; $P = 0.0499$). At 2 weeks after the surgery, the CBF of the nerve-compressed limb continued to be lower than that of the contralesional limb (129.6 ± 12.64 versus 195.0 ± 18.19; $P = 0.0014$) and the sham-operated limb (129.6 ± 12.64 versus 312.2 ± 16.45; $P < 0.0001$). Compared with the nonoperated limb in the sham group, the CBF of the nonoperated limb in the compression group was also decreased (195.0 ± 18.19 versus 349.9 ± 27.05; $P < 0.0001$). At 4 weeks, there was only a slight difference of the CBF between the nerve-compressed limb and the contralesional limb in the compression group (161.6 ± 17.29 versus 194.8 ± 25.37; $P = 0.0548$). However, both of them were significantly lower than in the corresponding limbs in the sham group (161.6 ± 17.29 versus 304.2 ± 21.93; $P = 0.0021$; and 194.8 ± 86.16 versus 327.3 ± 31.86; $P = 0.0080$). At 8 weeks, CBF of the nerve-compressed limb markedly improved in contrast with that at 2 weeks (204.8 ± 14.9 versus 129.6 ± 12.64; $P = 0.0132$), but the difference between the bilateral limbs in the compression group disappeared (204.8 ± 14.9 versus 200.2 ± 10.67; $P = 0.7118$), and both were diminished when compared with the corresponding limbs in the sham group (204.8 ± 14.9 versus 333.2 ± 20.02; $P = 0.0001$; and 200.2 ± 10.67 versus 359.3 ± 31.92; $P = 0.0001$) (Fig. 1).

The general blood flow seemed lower in the compression group in contrast to the sham group, which was observed from the tails, although this was not analyzed statistically.

Density of Sympathetic Fibers in Sciatic Nerve Decreased after Nerve Compression

Immunohistochemistry was used to determine the histologic changes of sympathetic fibers

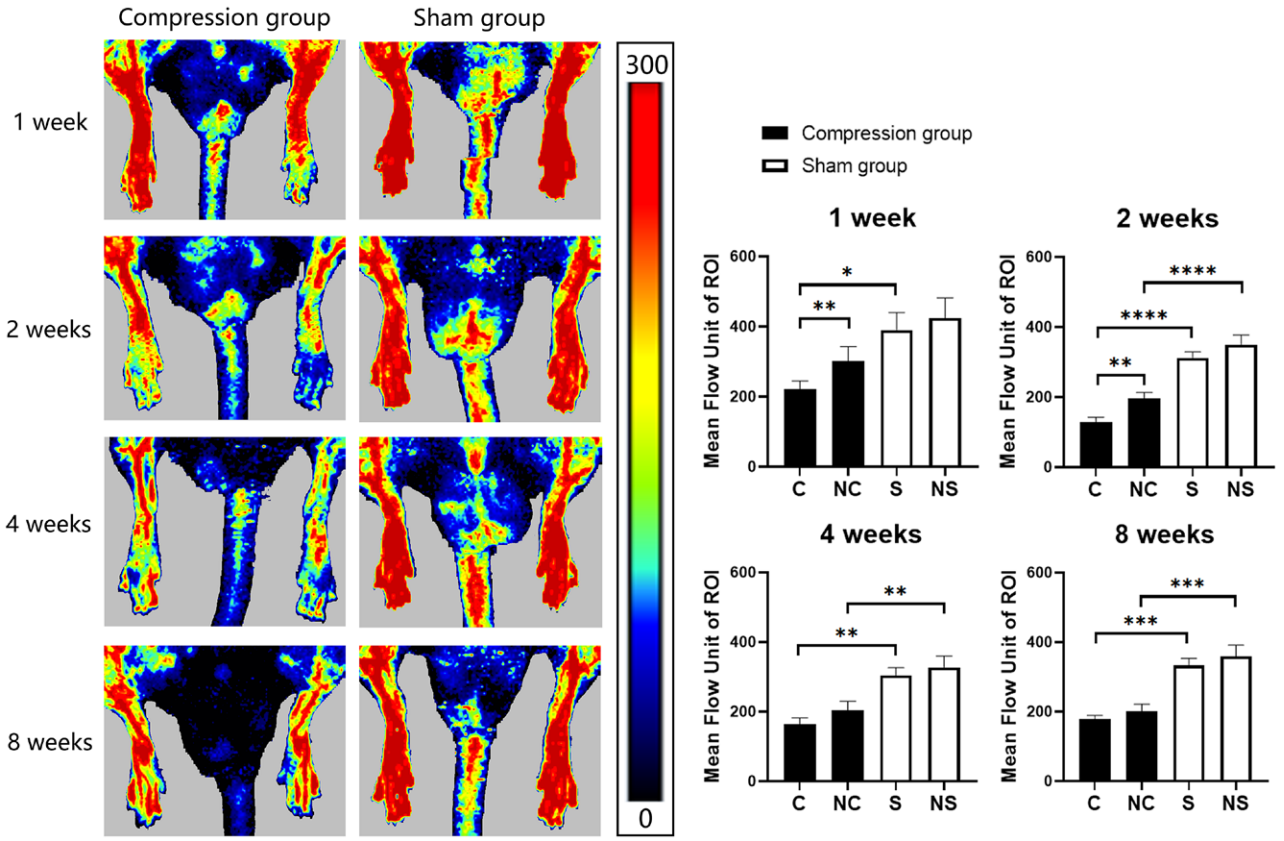

Fig. 1. Bilateral cutaneous blood flow as measured by laser Doppler imaging decreased after nerve compression. (*Left*) Representative laser Doppler images of the hind limbs in the compression group and sham group at 2, 4, and 8 weeks postoperatively. Areas with flow unit out of the range of the color scale are displayed as *deep red* or *black*. (*Right*) Quantitative analysis of laser Doppler images of the hind limbs in each group at 2, 4, and 8 weeks postoperatively. *$P < 0.05$; **$P < 0.01$; ***$P < 0.001$; ****$P < 0.0001$. *C*, compressed; *NC*, not compressed; *NS*, not sham-operated; *S*, sham-operated; ROI, region of interest (regions below the ankles).

in the sciatic nerve samples at 2, 4, and 8 weeks after the surgery.

In the compression group, the intraneural density of sympathetic fibers (INDSF) of the lesional side decreased significantly compared with the contralesional side at 2 weeks (1.435% ± 0.166% versus 3.067% ± 0.237%; $P < 0.0001$) and 4 weeks (1.760% ± 0.213% versus 3.338% ± 0.164%; $P = 0.0001$) after nerve compression. This difference vanished at 8 weeks (1.418% ± 0.079% versus 1.540% ± 0.148%; $P = 0.4849$). In contrast to the sham group, INDSF of the compressed nerve was significantly lower than in the sham-operated nerve at 2 weeks (1.435% ± 0.166% versus 3.068% ± 0.175%; $P = 0.0002$), 4 weeks (1.760% ± 0.213% versus 3.781% ± 0.339%; $P < 0.0001$), and 8 weeks (1.418% ± 0.079% versus 3.477% ± 0.176%; $P < 0.0001$). Compared with the corresponding limb in the sham group, INDSF in the contralesional nerve of the compression group also diminished at 8 weeks after the compression (1.540% ± 0.148% versus 3.028% ± 0.220%; $P < 0.0001$), although there was no difference at 2 weeks (3.067% ± 0.237% versus 3.241% ± 0.118%; $P > 0.9999$) or 4 weeks (3.338% ± 0.164% versus 3.766% ± 0.226%; $P > 0.9999$) (Fig. 2).

Unmyelinated Fibers Degenerated after Nerve Compression

At 2, 4, and 8 weeks after nerve compression, transmission electron microscopy was used to investigate the ultrastructural changes of unmyelinated fibers. Two weeks after the surgery, axon swelling and discontinuity of axon membrane were observed in the samples of compressed sciatic nerves. At 4 weeks, some axons in the compressed nerve samples had shrunk significantly, with a smaller overall diameter than the contralesional side (5.011 ± 0.329 versus 9.115 ± 0.362; $P < 0.0001$) and the sham-operated side (5.011 ± 0.329 versus 8.577 ± 0.197; $P < 0.0001$). Multiple

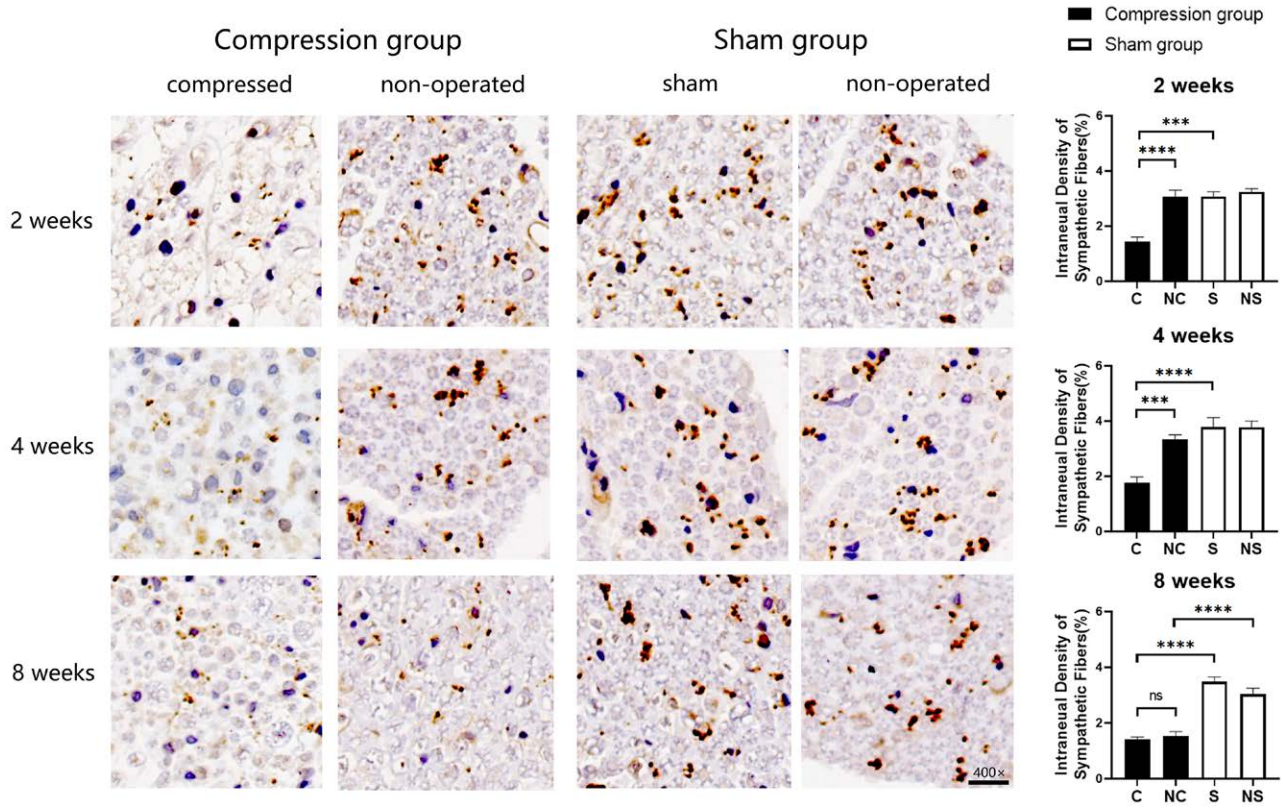

Fig. 2. Diminished bilateral INDSF after nerve compression. (*Left*) Representative images of dopamine β-hydroxylase–labeled sympathetic fibers in the sciatic nerve at 2, 4, and 8 weeks postoperatively (400×). (*Right*) Semiquantitative analysis of INDSF of hind limbs in all groups at 2, 4, and 8 weeks postoperatively. ***$P < 0.001$; ****$P < 0.0001$. *C*, compressed; *NC*, not compressed; *NS*, not sham-operated; *S*, sham-operated.

axons within one cytoplasmic domain of Remak cell were also found. At 8 weeks, axon loss was found in the compressed nerve specimens. Some axons lost the envelopment of Remak cells. The average diameter of the residual axons was equal to the contralesional side and sham-operated side. At 8 weeks, although there was no statistically significant difference in the diameter of the overall axons, axon swelling and shrinking also could be observed in the contralesional nerve samples, whereas axons were morphologically normal at 2 and 4 weeks. These changes, which indicate ultrastructural degeneration of unmyelinated fibers, were not observed in the sham group at any time point (Figs. 3 and 4).

DISCUSSION

The autonomic function anomalies of nerve compression, especially changes of cutaneous microcirculation, have not been well studied. Researchers have found a decreased vascular neural reaction of the affected paw in a rat sciatic nerve compression model, which was ameliorated after decompression.[17] Doppler ultrasonography revealed vasomotor dysfunction in digital arteries in patients with carpal tunnel syndrome.[18,19] It was also reported that the dorsal transcutaneous pressure of oxygen ($TcPO_2$) of the foot evidently improved after tarsal tunnel decompression.[14] Raynaud phenomenon, characterized by episodic color changes associated with paresthesia and throbbing of the digits, was also found to be more prevalent in patients with carpal tunnel syndrome than in the general population,[20,21] and can be relieved by surgical nerve decompression.[22] These findings suggested that impaired microcirculation of the innervated skin may occur after nerve compression.

We used a laser Doppler imaging system to measure the CBF of rat hind limbs. At 1 and 2 weeks after sciatic nerve compression, the CBF of the nerve-compressed limb decreased significantly. Beyond our initial hypothesis, at 2 weeks, the CBF of the contralesional limb also was reduced when compared with the corresponding limb in the sham group, although it was still higher than that of the lesional side. At 4 and 8 weeks after nerve

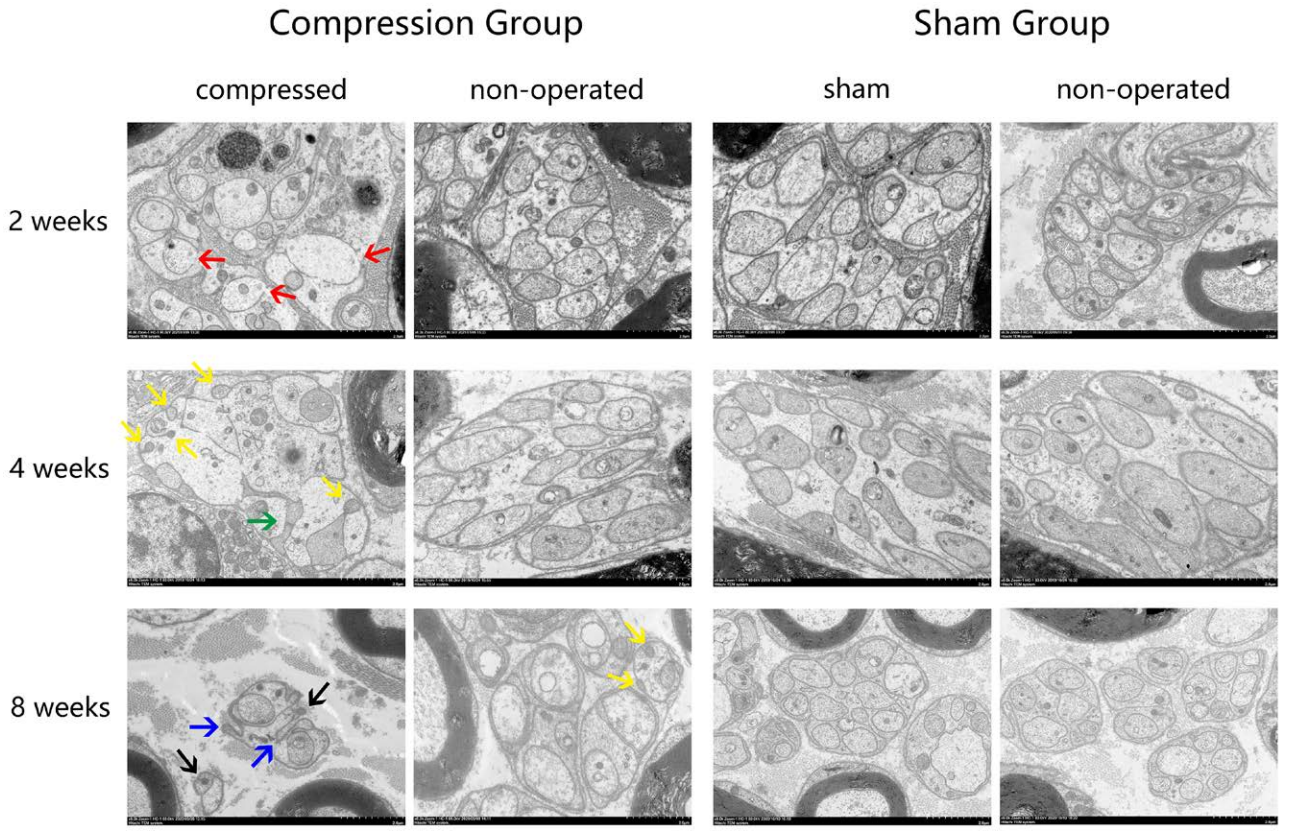

Fig. 3. Representative images of unmyelinated fibers of sciatic nerve samples at 2, 4, and 8 weeks after nerve compression captured by transmission electron microscopy (6000×). *Red arrows*: discontinuity of axon membrane. *Yellow arrows*: shrunken axons. *Green arrow*: multiple axons in one cytoplastic domain. *Blue arrows*: axon loss. *Black arrows*: loss of Remak cell envelopment.

compression, the difference in CBF between the two sides in the compression group disappeared, but CBF of both limbs remained lower than the corresponding limbs in the sham group.

Some relevant clinical studies explained this phenomenon from the aspect of surgical nerve decompression. A study found tyrosine hydroxylase–positive staining surrounding the vasculature in specimens from epineurectomy of the tibial nerve during decompression surgery.[23] The authors believed that the epineurectomy could provide a localized sympathectomy to the posterior tibial artery (PTA). However, no correlation between epineurectomy and sympathectomy of the PTA can be established because the sympathetic fibers found in the specimen should be innervating the nourishing vessels of the nerve itself rather than the PTA. Some authors considered that increased microcirculation was attributable to decompression of the vessels that are compressed anatomically by the swollen nerve.[14] However, a study using Doppler ultrasonography to evaluate the major arteries of the foot before and after nerve decompression revealed an improvement of pulsatility index, resistance index, and flow volume of dorsalis pedis and PTA, whereas the luminal cross-sectional area of the arteries did not change.[24] The outcomes indicated that the improvement of the arterial blood flow was independent of decompression of the large arteries. In an investigation into patients with diabetic peripheral neuropathy and peripheral arterial diseases, the CBF was found significantly but not completely restored after successful revascularization,[25] which also suggested that neural dysfunction was associated with the impaired cutaneous microcirculation despite the coexisting peripheral arterial diseases. The outcome of the current study supports this hypothesis as the major arteries of the hind limb are not adjacent to the sciatic nerve. Therefore, we can infer that neural dysfunction should be responsible for the injured cutaneous microcirculation after nerve compression.

In the current study, immunohistochemistry revealed a marked reduction of INDSF in the compressed nerve during the entire course of the study after nerve compression. Unexpectedly, INDSF in

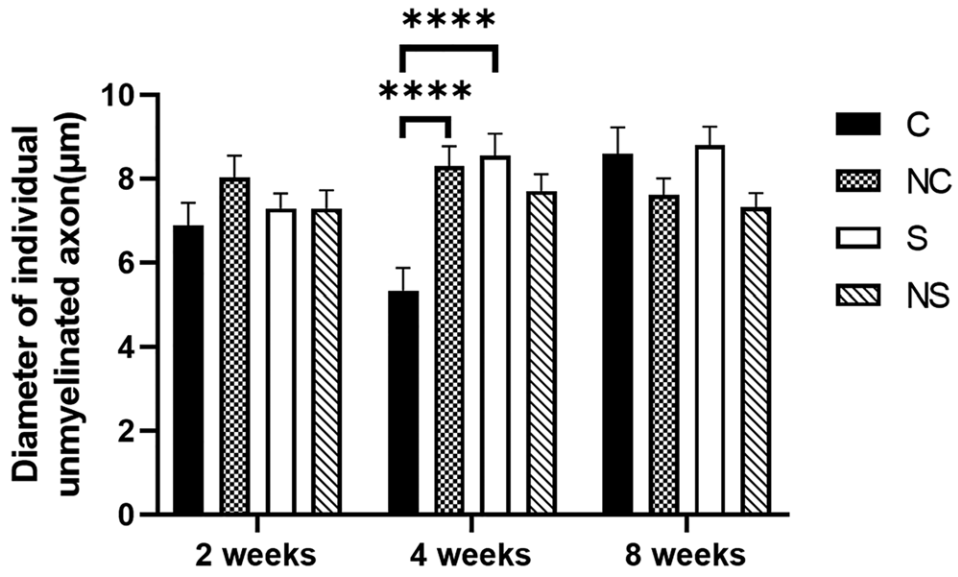

Fig. 4. Diameter of individual unmyelinated axons of the two groups at different time points. ****$P < 0.0001$. *C*, compressed; *NC*, not compressed; *NS*, not sham-operated; *S*, sham-operated.

the contralesional samples also were reduced at 8 weeks after the compression. At 2 weeks after the compression, axon swelling and discontinuity of axon membrane were observed by transmission electron microscopy. At 4 weeks, significant axon shrinking and multiple axons within one cytoplasmic domain of Remak cell were displayed, and axon loss was found at 8 weeks. These features indicated degeneration of unmyelinated fibers, in accordance with previous reports.[26,27] Axon swelling and shrinkage also were observed in the contralesional nerve samples at 8 weeks, whereas they were morphologically normal at 2 and 4 weeks. We presume that more classical degenerative features (e.g., axon loss) could be found in the contralesional nerve samples with a longer period of observation. Although it was impossible to differentiate sympathetic fibers from other categories of unmyelinated fibers by transmission electron microscopy, it can be inferred that the sympathetic axons also underwent the same changes.

There is increasing evidence that after peripheral nerve injury, the uninjured contralateral nerve is also affected.[28] A marked reduction of intraepidermal nerve fiber density was found in different nerve injury animal models, such as unilateral sciatic nerve compression,[28] unilateral chronic constriction injury of sciatic nerve,[29] and unilateral cutting plus ligation of tibial nerve model,[30] which was also found in human skin biopsy.[31] It can also present as a decreased reactivity to noxious stimulation.[32] The bilateral affected CBF, bilateral decreased sympathetic fibers, and bilateral degenerative features of unmyelinated fibers revealed by our study validate the previous findings. These histologic changes may explain why some patients with unilateral nerve injury developed bilateral symptoms.[33,34]

Regulation of cutaneous blood flow is achieved by alteration in the diameter of peripheral arterioles, which is predominantly regulated by the sympathetic vasomotor fibers.[18] In a thermoneutral environment, neural regulation of peripheral blood vessels is entirely by sympathetic vasoconstriction through adrenergic receptors,[34,35] whereas vasodilator nerve fibers are not functional in most peripheral blood vessels.[36] Therefore, the degeneration and decrease of sympathetic fibers should lead to vascular denervation and subsequent dilation of blood vessels, increasing the CBF. However, there was an obvious contradiction between the laser Doppler imaging outcomes and immunohistochemistry outcomes in our study. We hypothesize that the voltage-gated sodium channel (VGSC) might be involved in this phenomenon. The VGSC is the most important ion channel required for neuronal cells to generate excitability and execute normal physiologic functions.[37] Expression of VGSC is highly active in peripheral nerves and would change massively after nerve injury.[38–41] The elevated expression of VGSC is regarded to be responsible for neurogenic pain. For example, the substantiality of trigeminal neuralgia is widely considered to be a

sort of hyperexcitability of ectopic action potentials,[42–44] which can be attenuated by blockers of VGSC.[45–47] Its role in neuropathic pain after spinal cord injury has been proven.[48]

We presume that nerve compression induced a potent hyperexcitability or massive spontaneous action potentials of VGSC on sympathetic fibers in the early phase. Although the INDSF decreased from the early phase, this elevated electrical activity of VGSC still resulted in an increased sympathetic vasoconstriction tone and subsequent contraction of blood vessels in the skin, which decreased CBF. As nerve compression advanced, the progressive degeneration of sympathetic fibers led to a progressive denervation of vasculature, causing a gradual microvascular dilation. Therefore, the gradual recovery of CBF in the later phase might be a false impression of spontaneous repair of sympathetic fibers. This hypothesis may also explain the reduced vasoneural reaction and the insignificant result under capillaroscopy in long-term nerve compression.[17,18,49] Moreover, expression of VGSC was also found in the smooth muscle cells of various blood vessels in normal or disease conditions.[50–55] The physiology of blood vessels can be stimulated or inhibited by VGSC-targeted chemicals,[55–58] but the role of VGSC was less defined. Further investigation into the mechanism of this paradoxical phenomenon is needed.

Nerve decompression is increasingly being accepted as an effective method to prevent diabetic foot ulcers.[9–13] Its effect on ulcer healing, however, has not been well understood. The outcomes of this study provide evidence that nerve compression can reduce CBF, which may further expose the skin of the innervated domain to the risk of ulcer formation or delay wound-healing. Although this effect may not be obvious in the general population, the complicated pathophysiology in diabetic patients may magnify this negative effect, as autonomic dysfunction has been proved strongly relevant to the diabetic foot.[59] Therefore, our findings could provide a supplement to the theoretical basis of nerve decompression for preventing ulcer recurrence. Prompt nerve decompression correcting the significantly decreased blood flow would be beneficial for wound healing in patients with existing ulcers. Further studies are needed to validate the effects of nerve compression on wound healing and the benefits of early nerve decompression on ulcer healing.

CONCLUSIONS

The current study revealed that the cutaneous microcirculation of bilateral hind limbs was decreased in a rat unilateral nerve compression model. Histologic outcomes indicated a degeneration of sympathetic fibers in the bilateral sciatic nerves. These changes between the hind limbs in each experimented individual were not synchronous and emerged later in the contralesional side. These results may validate the importance and broaden the indication of surgical nerve decompression in preventing or treating foot ulcers.

Zenggan Chen, PhD
Zhongshan Hospital
Fudan University
180 Fenglin Road
Shanghai 200032, China
chen.zenggan@zs-hospital.sh.com

Jian Zhang, PhD
Zhongshan Hospital
Fudan University
180 Fenglin Road
Shanghai 200032, China
zhang.jian@zs-hospital.sh.com

ACKNOWLEDGMENT

This research was supported by the National Natural Science Foundation of China (grant 81870965). The authors thank Yiji Tu and Zhenqing Wang for their technical assistance.

REFERENCES

1. Jacobson L, Dengler J, Moore AM. Nerve entrapments. *Clin Plast Surg.* 2020;47:267–278.
2. Linscheid RL, Peterson LF, Juergens JL. Carpal-tunnel syndrome associated with vasospasm. *J Bone Joint Surg Am.* 1967;49:1141–1146.
3. Verghese J, Galanopoulou AS, Herskovitz S. Autonomic dysfunction in idiopathic carpal tunnel syndrome. *Muscle Nerve* 2000;23:1209–1213.
4. Zyluk A, Kosowiec L. Regionalne zaburzenia układu współczulnego w zespole kanału nadgarstka: przeglad piśmiennictwa [Regional sympathetic disturbances in carpal tunnel syndrome: a review]. *Chir Narzadow Ruchu Ortop Pol.* 2008;73:30–36.
5. Dellon AL. Susceptibility of nerve in diabetes to compression: implications for pain treatment. *Plast Reconstr Surg.* 2014;134(4 Suppl 2):142S–150S.
6. Armstrong DG, Boulton AJM, Bus SA. Diabetic foot ulcers and their recurrence. *N Engl J Med.* 2017;376:2367–2375.
7. Palande DD, Azhaguraj M. Surgical decompression of posterior tibial neurovascular complex in treatment of certain chronic plantar ulcers and posterior tibial neuritis in leprosy. *Int J Lepr Other Mycobact Dis.* 1975;43:36–40.
8. Hollis Caffee H. Treatment of diabetic neuropathy by decompression of the posterior tibial nerve. *Plast Reconstr Surg.* 2000;106:813–815.

9. Albers JW, Jacobson R. Decompression nerve surgery for diabetic neuropathy: a structured review of published clinical trials. *Diabetes Metab Syndr Obes.* 2018;11:493–514.
10. Aszmann O, Tassler PL, Dellon AL. Changing the natural history of diabetic neuropathy: incidence of ulcer/amputation in the contralateral limb of patients with a unilateral nerve decompression procedure. *Ann Plast Surg.* 2004;53:517–522.
11. Sarmiento S, Pierre JA Jr, Dellon AL, Frick KD. Tibial nerve decompression for the prevention of the diabetic foot: a cost-utility analysis using Markov model simulations. *BMJ Open* 2019;9:e024816.
12. Nickerson DS, Rader AJ. Nerve decompression after diabetic foot ulceration may protect against recurrence: a 3-year controlled, prospective analysis. *J Am Podiatr Med Assoc.* 2014;104:66–70.
13. Agarwal P, Sharma B, Sharma D. Tarsal tunnel release restores sensations in sole for diabetic sensorimotor polyneuropathy. *J Clin Orthop Trauma* 2020;11:442–447.
14. Trignano E, Fallico N, Chen HC, et al. Evaluation of peripheral microcirculation improvement of foot after tarsal tunnel release in diabetic patients by transcutaneous oximetry. *Microsurgery* 2016;36:37–41.
15. Bickel A, Butz M, Schmelz M, Handwerker HO, Neundörfer B. Density of sympathetic axons in sural nerve biopsies of neuropathy patients is related to painfulness. *Pain* 2000;84:413–419.
16. Matsubayashi T, Cho KH, Jang HS, Murakami G, Yamamoto M, Abe S. Significant differences in sympathetic nerve fiber density among the facial skin nerves: a histologic study using human cadaveric specimens. *Anat Rec (Hoboken)* 2016;299:1054–1059.
17. Pelletier J, Fromy B, Morel G, Roquelaure Y, Saumet JL, Sigaudo-Roussel D. Chronic sciatic nerve injury impairs the local cutaneous neurovascular interaction in rats. *Pain* 2012;153:149–157.
18. Galea LA, Mercieca A, Sciberras C, Gatt R, Schembri M. Evaluation of sympathetic vasomotor fibres in carpal tunnel syndrome using continuous wave Doppler ultrasonography. *J Hand Surg Br.* 2006;31:306–310.
19. Wilder-Smith EP, Fook-Chong S, Chew SE, Chow A, Guo Y. Vasomotor dysfunction in carpal tunnel syndrome. *Muscle Nerve* 2003;28:582–586.
20. Pal B, Keenan J, Misra HN, Moussa K, Morris J. Raynaud's phenomenon in idiopathic carpal tunnel syndrome. *Scand J Rheumatol.* 1996;25:143–145.
21. Chung MS, Gong HS, Baek GH. Prevalence of Raynaud's phenomenon in patients with idiopathic carpal tunnel syndrome. *J Bone Joint Surg Br.* 1999;81:1017–1019.
22. Chung MS, Gong HS, Baek GH. Raynaud's phenomenon in idiopathic carpal tunnel syndrome: postoperative alteration in its prevalence. *J Bone Joint Surg Br.* 2000;82:818–819.
23. Blount AL, Peled ZM, Dexter EL, Nagle RB, Maloney CT, Dellon AL. Sympathetic nerves in the tarsal tunnel: implications for blood flow in the diabetic foot. *Plast Reconstr Surg.* 2008;122:188–191.
24. Tekin F, Ağladioğlu K, Sürmeli M, et al. The ultrasonographic evaluation of hemodynamic changes in patients with diabetic polyneuropathy after tarsal tunnel decompression. *Microsurgery* 2015;35:457–462.
25. Arora S, Pomposelli F, LoGerfo FW, Veves A. Cutaneous microcirculation in the neuropathic diabetic foot improves significantly but not completely after successful lower extremity revascularization. *J Vasc Surg.* 2002;35:501–505.
26. Orita S, Henry K, Mantuano E, et al. Schwann cell LRP1 regulates Remak bundle ultrastructure and axonal interactions to prevent neuropathic pain. *J Neurosci.* 2013;33:5590–5602.
27. Yvon A, Faroni A, Reid AJ, Lees VC. Selective fiber degeneration in the peripheral nerve of a patient with severe complex regional pain syndrome. *Front Neurosci.* 2018;12:207.
28. Hsieh CH, Jeng SF, Lu TH, Chen YC, Hsieh MW, Chen SS. Loss of small fibers in entrapment neuropathy and their regeneration after surgical decompression in a rat model. *J Neurotrauma* 2007;24:1658–1666.
29. Lindenlaub T, Sommer C. Epidermal innervation density after partial sciatic nerve lesion and pain-related behavior in the rat. *Acta Neuropathol.* 2002;104:137–143.
30. Oaklander AL, Brown JM. Unilateral nerve injury produces bilateral loss of distal innervation. *Ann Neurol.* 2004;55:639–644.
31. Oaklander AL, Romans K, Horasek S, Stocks A, Hauer P, Meyer RA. Unilateral postherpetic neuralgia is associated with bilateral sensory neuron damage. *Ann Neurol.* 1998;44:789–795.
32. Vissers K, Adriaensen H, De Coster R, De Deyne C, Meert TF. A chronic-constriction injury of the sciatic nerve reduces bilaterally the responsiveness to formalin in rats: a behavioral and hormonal evaluation. *Anesth Analg.* 2003;97:520–525.
33. Kozin F, Genant HK, Bekerman C, McCarty DJ. The reflex sympathetic dystrophy syndrome: II: Roentgenographic and scintigraphic evidence of bilaterality and of periarticular accentuation. *Am J Med.* 1976;60:332–338.
34. Wenderhold W, Kunkel M, Eicke BM, Reimers CD. Continuous wave Doppler ultrasound for evaluation of vasomotor tone of the radial artery. *Eur J Ultrasound* 1999;10:11–20.
35. Estañol B, Corona MV, Elías Y, Téllez-Zenteno JF, Infante O, García-Ramos G. Sympathetic co-activation of skin blood vessels and sweat glands. *Clin Auton Res.* 2004;14:107–112.
36. Chao CY, Gl C. Microvascular dysfunction in diabetic foot disease and ulceration. *Diabetes Metab Res Rev.* 2009;25:604–614.
37. Wang J, Ou SW, Wang YJ. Distribution and function of voltage-gated sodium channels in the nervous system. *Channels (Austin)* 2017;11:534–554.
38. Rizzo MA, Kocsis JD, Waxman SG. Selective loss of slow and enhancement of fast Na+ currents in cutaneous afferent dorsal root ganglion neurones following axotomy. *Neurobiol Dis.* 1995;2:87–96.
39. Dib-Hajj SD, Fjell J, Cummins TR, et al. Plasticity of sodium channel expression in DRG neurons in the chronic constriction injury model of neuropathic pain. *Pain* 1999;83:591–600.
40. Black JA, Cummins TR, Plumpton C, et al. Upregulation of a silent sodium channel after peripheral, but not central, nerve injury in DRG neurons. *J Neurophysiol.* 1999;82:2776–2785.
41. Kim CH, Oh Y, Chung JM, Chung K. The changes in expression of three subtypes of TTX sensitive sodium channels in sensory neurons after spinal nerve ligation. *Brain Res Mol Brain Res.* 2001;95:153–161.
42. Burchiel KJ, Wyler AR. Ectopic action potential generation in peripheral trigeminal axons. *Exp Neurol.* 1978;62:269–281.
43. Burchiel KJ. Abnormal impulse generation in focally demyelinated trigeminal roots. *J Neurosurg.* 1980;53:674–683.
44. Fromm GH, Terrence CF, Maroon JC. Trigeminal neuralgia: current concepts regarding etiology and pathogenesis. *Arch Neurol.* 1984;41:1204–1207.
45. Buttermore ED, Thaxton CL, Bhat MA. Organization and maintenance of molecular domains in myelinated axons. *J Neurosci Res.* 2013;91:603–622.
46. Henry MA, Luo S, Foley BD, Rzasa RS, Johnson LR, Levinson SR. Sodium channel expression and localization at demyelinated sites in painful human dental pulp. *J Pain* 2009;10:750–758.

47. Zhou QM, Zhong J, Jiao W, et al. The role of autonomic nervous system in the pathophysiology of hemifacial spasm. *Neurol Res.* 2012;34:643–648.
48. Hains BC, Klein JP, Saab CY, Craner MJ, Black JA, Waxman SG. Upregulation of sodium channel Nav1.3 and functional involvement in neuronal hyperexcitability associated with central neuropathic pain after spinal cord injury. *J Neurosci.* 2003;23:8881–8892.
49. Zyluk A, Kosovets L. An assessment of the sympathetic function within the hand in patients with carpal tunnel syndrome. *J Hand Surg Eur Vol.* 2010;35:402–408.
50. Berra-Romani R, Blaustein MP, Matteson DR. TTX-sensitive voltage-gated Na+ channels are expressed in mesenteric artery smooth muscle cells. *Am J Physiol Heart Circ Physiol.* 2005;289:H137–H145.
51. Mironneau J, Martin C, Arnaudeau S, et al. High-affinity binding sites for [3H]saxitoxin are associated with voltage-dependent sodium channels in portal vein smooth muscle. *Eur J Pharmacol.* 1990;184:315–319.
52. Meguro K, Iida H, Takano H, et al. Function and role of voltage-gated sodium channel NaV1.7 expressed in aortic smooth muscle cells. *Am J Physiol Heart Circ Physiol.* 2009;296:H211–H219.
53. Platoshyn O, Remillard CV, Fantozzi I, Sison T, Yuan JX. Identification of functional voltage-gated Na(+) channels in cultured human pulmonary artery smooth muscle cells. *Pflugers Arch.* 2005;451:380–387.
54. Quignard JF, Ryckwaert F, Albat B, Nargeot J, Richard S. A novel tetrodotoxin-sensitive Na+ current in cultured human coronary myocytes. *Circ Res.* 1997;80:377–382.
55. Saleh S, Yeung SY, Prestwich S, Pucovsky V, Greenwood I. Electrophysiological and molecular identification of voltage-gated sodium channels in murine vascular myocytes. *J Physiol.* 2005;568(Pt 1):155–169.
56. Bocquet A, Sablayrolles S, Vacher B, Le Grand B. F 15845, a new blocker of the persistent sodium current, prevents consequences of hypoxia in rat femoral artery. *Br J Pharmacol.* 2010;161:405–415.
57. Fort A, Cordaillat M, Thollon C, et al. New insights in the contribution of voltage-gated Na(v) channels to rat aorta contraction. *PLoS One* 2009;4:e7360.
58. Ho WS, Davis AJ, Chadha PS, Greenwood IA. Effective contractile response to voltage-gated Na+ channels revealed by a channel activator. *Am J Physiol Cell Physiol.* 2013;304:C739–C747.
59. Forst T, Pfützner A, Kann P, Lobmann R, Schäfer H, Beyer J. Association between diabetic-autonomic-C-fibre-neuropathy and medial wall calcification and the significance in the outcome of trophic foot lesions. *Exp Clin Endocrinol Diabetes* 1995;103:94–98.